

Persilylated Phosphoranyl Radicals: The First Persistent Noncyclic Phosphoranyl Radicals

Yves Berchadsky,^[a, b] Christiane Bernard-Henriet,^[a] Jean-Pierre Finet,^[a]
Robert Lauricella,^[a, c] Sylvain R. A. Marque,^{*[a]} and Paul Tordo^[a]

Abstract: Persistent noncyclic phosphoranyl radicals have been prepared and observed by electron paramagnetic resonance (EPR) for the first time. They were obtained by UV-photolysis of a solution containing a bis(trialkylsilyl) peroxide (R = Me, Et) and a tris(trialkylsilyl) phosphite (R = Me, Et, *i*Pr). EPR parameters ($a_p \approx 100$ mT) are typical of phosphoranyl

radicals exhibiting a trigonal-bipyramidal structure, with the odd electron in an equatorial site. Analysis of the pseudo-first-order decay shows that

Keywords: electron paramagnetic resonance • kinetics • phosphoranyl radicals • radical reactions • reactive intermediates

these phosphoranyl radicals decay by S_H2 homolytic substitution on the bis-(trialkylsilyl) peroxide and by loss of a trialkylsilyloxy radical (α -scission reaction). Both the S_H2 and α -scission reactions depend on the steric bulk of the alkyl groups, that is, the bulkier the alkyl group, the slower the S_H2 and α -scission reactions.

Introduction

Phosphoranyl radicals were first observed more than 35 years ago,^[1,2] and since then their structures and reactivities have been extensively studied.^[3–10] Most studies on these radicals have dealt with their application in synthesis.^[11] However, in recent years, their physical properties have induced a keen interest among polymer chemists^[12,13] and in the magnetic resonance community with regard to their application in dynamic nuclear polarization (DNP).^[14,15] Basically, DNP is the amplification of NMR signals of nuclei in solvent molecules.^[16] This amplification is obtained through coupling of the nuclear spin system of the solvent with the electronic spin system of a highly persistent (or stable) free

radical present as a solute. The intensity of the DNP is directly proportional to the amplitude of the hyperfine coupling constant a , and also depends on several other factors such as the temperature T , the magnitude of the electron paramagnetic resonance line width ΔH_{EPR} , the radical concentration, and the efficiency factor f , which gives a measure of the influence of the unpaired electronic spin on the longitudinal relaxation time of the solvent nuclei.^[17]

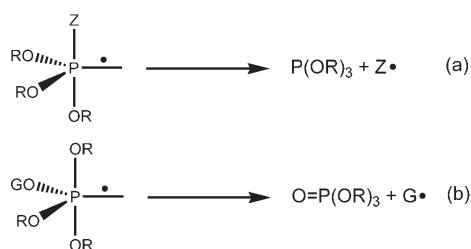
Thus, because of the strong phosphorus hyperfine coupling constant a_p , most free radicals centred on phosphorus are potentially of great interest for DNP. Among the various structural types of known phosphorus-centred free radicals, phosphoranyl radicals show the highest potential for application in DNP because of their large a_p values ($a_p > 80$ mT)—due to their trigonal-bipyramidal (TBP) geometry, involving high s character in the SOMO, and of their relatively narrow ΔH_{EPR} ($\Delta H_{EPR} \approx 0.15$ mT), and of their good efficiency factor f ($f = 0.7$).^[18] However, application of phosphoranyl radicals in DNP is impeded by their short half-life times (typically, $t_{1/2} < 1$ s at room temperature).^[14,15,18] Phosphoranyl radicals are generally considered as transient species and their main decay processes occur through two pathways: α -scission yielding a phosphite (Scheme 1a) or β -scission yielding a phosphate (Scheme 1b).^[3–11]

The persistence of phosphoranyl radicals is significantly increased when the phosphorus atom is incorporated into a ring (Scheme 2), but still not sufficiently to permit DNP ap-

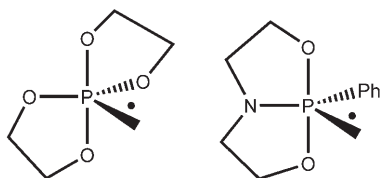
[a] Dr. Y. Berchadsky, Dr. C. Bernard-Henriet, Dr. J.-P. Finet, Dr. R. Lauricella, Dr. S. R. A. Marque, Prof. P. Tordo
Universités d'Aix-Marseille 1–3, CNRS - UMR 6517, Faculté des Sciences de St. Jérôme, case 542, Avenue Escadrille Normandie-Niemen, 13397 Marseille Cedex 20 (France)
E-mail: sylvain.marque@up.univ-mrs.fr

[b] Dr. Y. Berchadsky
Present address: Fédération de Recherche des Sciences Chimiques de Marseille, CNRS FR1739, Faculté des Sciences de St. Jérôme, case A62, Avenue Escadrille Normandie-Niemen, 13397 Marseille Cedex 20 (France)

[c] Dr. R. Lauricella
Present address: Université d'Aix-Marseille 1–3, JE TRACES, case 512, Avenue Escadrille Normandie-Niemen, 13397 Marseille Cedex 20 (France)

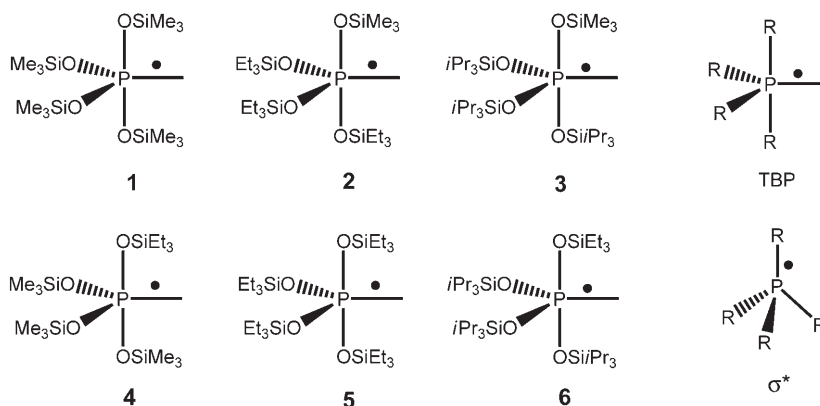


Scheme 1. Fragmentation processes.



Scheme 2. Structures of typical cyclic phosphoranyl radicals.

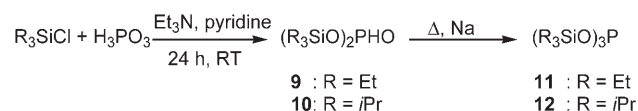
plications.^[7–10,14] Assuming that the occurrence of decay processes is mainly related to the strength of the bonds involved in the fragmentation processes in terms of BDE (bond dissociation energy), strengthening of the P–Z and O–G bonds should considerably increase the lifetime of the phosphoranyl radicals. Thus, we present herein the generation of persilylated phosphoranyl radicals **1–6** (Scheme 3) and an EPR analysis of their structures and reactivities. These compounds exhibit a sequence of two contiguous strong bonds: O–Si (BDE \approx 513 kJ mol⁻¹)^[19] and O–P (BDE = 336 kJ mol⁻¹).^[4]

Scheme 3. Structures of phosphoranyl radicals **1–6**.

Abstract in French: Des radicaux phosphoranyl noncycliques persistants ont été détectés pour la première fois par résonance paramagnétique électronique (RPE). Ils sont préparés, *in situ* dans la cavité du spectromètre, par irradiation UV d'une solution contenant un peroxyde de bis(trialkylsilyl) ($R = \text{Me}, \text{Et}$) et un phosphite de tris(trialkylsilyl) ($R = \text{Me}, \text{Et}, \text{iPr}$). Les paramètres de RPE ($a_p \approx 0.1 \text{ T}$) sont caractéristiques d'un radical présentant une structure bipyramidale à base triangulaire. L'étude cinétique montre que les radicaux phosphoranyl disparaissent par réaction de substitution homolytique du second ordre (S_H2) sur le peroxyde de bis(trialkylsilyl) et par perte d'un radical trialkylsilyloxyl (α -scission). Ces réactions sont d'autant plus lentes que le groupement alkyl est volumineux.

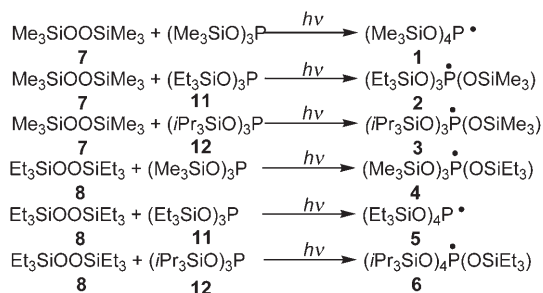
Results and Discussion

Generation of the phosphoranyl radicals: The phosphoranyl radicals were generated by UV-irradiation (high-pressure 1000 W Xe-Hg arc lamp) of a solution containing the requisite silyl peroxide and silyl phosphite. The bis(trialkylsilyl) peroxides **7** and **8** were prepared as reported in the literature.^[20] However, purification of **8** proved tedious due to the presence of various side products, such as the corresponding triethylsilanol, hexaethylsiloxane, and triethylsilyl hydroperoxide, which have very close boiling points.^[21,22] The preparation of the phosphites **11** and **12** was carried out in two steps (Scheme 4) by an adaptation of the procedure of Sekine et al.^[23] In the first step, phosphonates **9** and **10** were prepared by silylation of phosphorous acid. In the second step, phosphonates **9** and **10** were reduced with sodium metal to afford the phosphites **11** and **12**, respectively. Care must be taken during the handling of **11** because of its high sensitivity to hydrolysis (hydrolysis was observed at temperatures above 18 °C).^[24]

Scheme 4. Preparation of tris(trialkylsilyl) phosphites **11** and **12**.

The phosphoranyl radicals **1–6** were generated in the EPR cavity by UV-irradiation of a mixture of the appropriate peroxide, **7** or **8**, with the appropriate phosphite, **11** or **12**, or with tris(trimethylsilyl) phosphite (Scheme 5).

Structure of the phosphoranyl radicals: The EPR spectra of all of the studied radicals (Table 1) featured a two-line signal with very large a_p (around 100 mT) and g factors of around 2.002, which are typical of phosphorus-centred radicals belonging to the phosphoranyl family (Figure 1).^[25–27] The values of a_p and g were not significantly influenced by the nature of the solvent (variations of only a few mT). The EPR spectra of the radicals bearing one odd ligand, **2–4** and



Scheme 5. Generation of phosphoranyl radicals **1–6**.

Table 1. ^{31}P hyperfine coupling constants, a_{P} , and Landé factors, g , for phosphoranyl radicals **1–6** in various solvents at 273 K.

Radicals	Solvents	$a_{\text{P}}^{[\text{a},\text{b}]}$ [mT]	$g^{[\text{a},\text{b}]}$
1	<i>n</i> -hexane	98.80	2.0018
	toluene	98.40	2.0017
2	<i>n</i> -hexane	99.70	2.0023
		(97.90)	(2.0034)
3	<i>n</i> -hexane	100.1	2.0032
		(99.00)	(2.0033)
	cyclopropane	99.90	2.0025
4		(99.20)	(2.0025)
	<i>n</i> -hexane ^[c]	99.70	2.0012
	toluene	99.60	2.0010
5	cyclopropane	99.60	2.0010
	<i>n</i> -hexane	104.5	2.0025
		(102.6)	(2.0026)
	toluene	104.7	2.0015
		(102.3)	(2.0008)
6	cyclopropane	104.5	2.0020
		(102.8)	(2.0020)
	<i>n</i> -hexane ^[c]	105.0	2.000
		(103.7)	(2.0038)
	toluene	105.4	2.0024
	(103.9)	(2.0027)	
	benzene	105.4	2.0024
		(103.9)	(2.0024)
	cyclopropane	104.8	2.0037
		(103.5)	(2.0037)

[a] a_{P} and g were obtained by applying the simulation program of A. Rockenbauer^[28] with the Breit–Rabi correction^[29] included. [b] Values for the minor species in parentheses. [c] Given in reference [18].

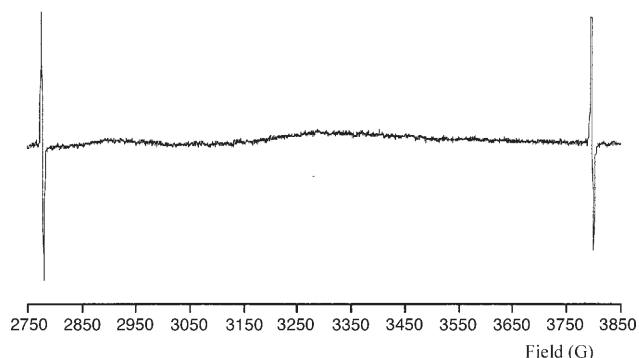


Figure 1. EPR spectrum of **5** in *n*-hexane at 273 K.

6, revealed the presence of a minor species (Figure 2) that also exhibited the features of a phosphoranyl radical. This results from an equilibrium between isomers having the odd

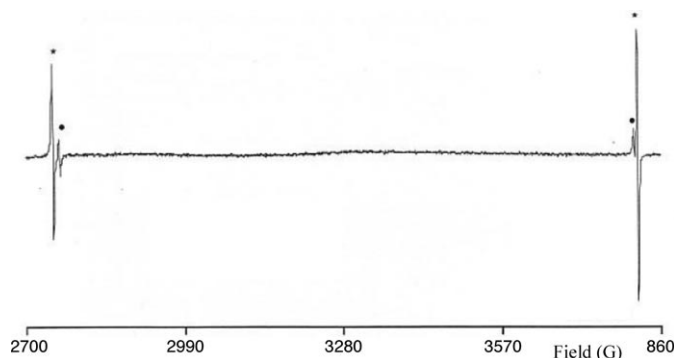
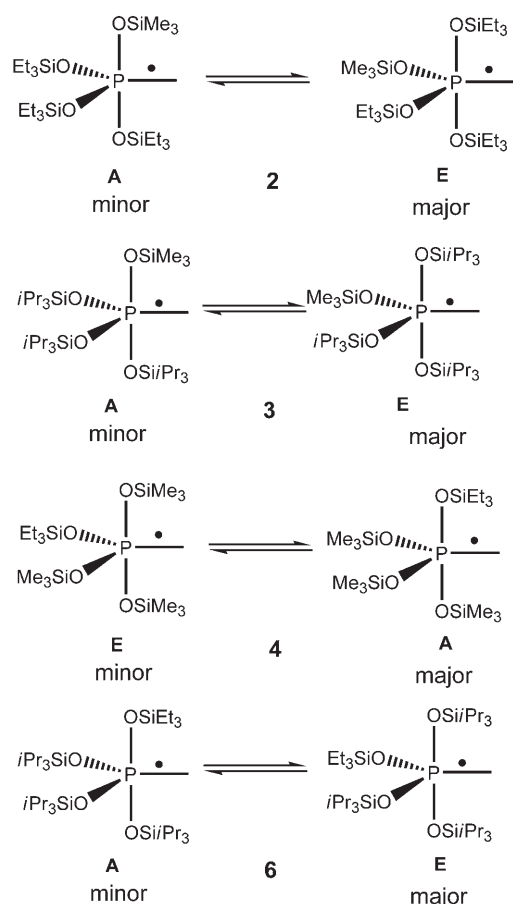


Figure 2. EPR spectrum of **3** in *n*-hexane at 273 K, showing signals due to the major species (equatorial isomer) (*) and the minor species (apical isomer) (●).

ligand in either an apical or an equatorial position (vide infra).^[4,7,9] The ratios of spin densities in the 3p and 3s orbitals, ρ_{3p}/ρ_{3s} , calculated from the anisotropic EPR spectra^[18] for **5** (1.97) and **6** (1.75) are typical of phosphoranyl radicals exhibiting TBP geometries.^[30,31] Therefore, as all of the observed radicals exhibit very large and close a_{P} values and similar g factors, TBP geometries with varying degrees of distortion can be assumed for both the major and minor species of the phosphoranyl radicals **1–6** (Scheme 3).

Assignment of the minor species observed for **2–4** and **6** to either an impurity or to the decay of the major species was ruled out for various reasons. The peroxides **7** and **8** and the phosphites **11** and **12** were carefully purified to attain a high level of purity (see Experimental Section). In the EPR experiments, the intensities of the signals of the minor and major species grew simultaneously when the light was switched on, whatever the experimental conditions (temperature, concentrations of the phosphites and peroxides, solvent, light intensity). Moreover, the minor signal appeared only in the case of those phosphoranyl radicals bearing one distinct ligand, and the minor and major species increased and decayed in a parallel fashion. On the other hand, the reversible evolution of the signal (vide infra) is a characteristic feature of a chemical exchange between ligands in apical and equatorial positions.^[32,33] Roberts et al. showed that the bulkiest substituents are located in the apical positions (apical bonds are longer than equatorial bonds and therefore the strain relief is greater), that the less strained isomer exhibits the largest a_{P} , and that the more electronegative ligands occupy the apical positions.^[7,34,35] In our series, we can assume that *i*Pr₃SiO, Et₃SiO, and Me₃SiO groups have essentially the same electron-withdrawing capacity^[36] and that the steric bulk decreases in the sequence *i*Pr₃SiO > Et₃SiO > Me₃SiO. In the case of radicals **3** and **6**, the isomer exhibiting the largest a_{P} , that is, the major species (equatorial isomer **E**), has two *i*Pr₃SiO groups in the apical positions and the Me₃SiO or Et₃SiO group, respectively, in an equatorial position. These isomers are in chemical exchange with the isomer having the Me₃SiO or Et₃SiO group in an apical position (apical isomer **A**) as shown in



Scheme 6. Chemical exchange processes for phosphoranyl radicals **2**, **3**, **4**, and **6**.

Scheme 6. The same behaviour should be observed for radicals **2** and **4**, as also shown in Scheme 6.

Temperature dependence of the EPR spectra of 3 and 6: Because of the high persistency of **3** and **6** (vide infra), the temperature dependence of their EPR spectra was easy to determine. A reversible change in the EPR lines with temperature (Figure 3) is a characteristic feature of a chemical exchange between two conformers.^[32,33] For phosphoranyl radicals **3** and **6**, the exchange occurs between ligands in equatorial (major species) and apical positions (minor species) (Scheme 6).

The Van't Hoff (Figure 4a) and Arrhenius (Figure 4b) parameters were determined by using Equation (1) and Equation (2), respectively (Table 2). Both the equilibrium constants, K , and the rate constants, k_{exc} , for the exchange were determined by applying the program of A. Rockenbauer.^[28]

$$\ln K_{\text{exc}} = \ln \frac{[\text{E}]}{[\text{A}]} = -\frac{\Delta H_{\text{exc}}}{R} \cdot \frac{1}{T} + \frac{\Delta S_{\text{exc}}}{R} \quad (1)$$

$$k = A \cdot \exp(-E_a/RT) \quad (2)$$

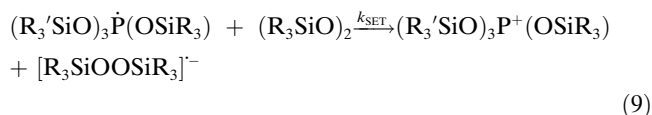
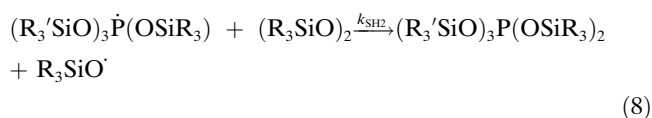
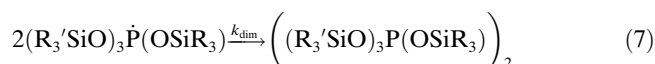
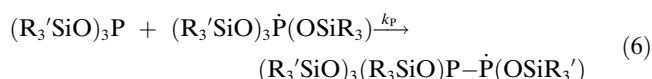
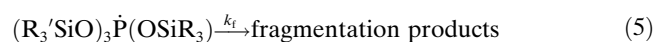
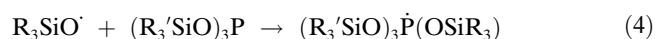
The thermodynamic parameters for the exchange (ΔH_{exc} and ΔS_{exc}) are small, indicating that the stability difference between the respective isomers is small, and they are close to the values reported in the literature for cyclic^[37] and acyclic^[33] phosphoranyl radicals. As expected, ΔH_{exc} is negative for the conversion from the apical isomer to the less hindered equatorial isomer. Furthermore, the equatorial isomer of **6** is slightly enthalpically favored over the equatorial isomer of **3**: $\Delta H_{\text{exc}}(\mathbf{6}) < \Delta H_{\text{exc}}(\mathbf{3})$ (Table 2). On the other hand, the negative values of ΔS_{exc} for **3** and **6** indicate that the equatorial isomer has a lower motion freedom than the apical isomer because of the steric congestion due to the presence of a bulky $i\text{Pr}_3\text{SiO}$ group in an equatorial position. Furthermore, the negative $\Delta\Delta S_{\text{exc}}$ [$\Delta S_{\text{exc}}(\mathbf{6}) < \Delta S_{\text{exc}}(\mathbf{3})$] suggests that the equatorial isomer of **6** has a lower motion freedom than the equatorial isomer of **3**, probably because of the larger internal strain due to the greater bulk of the Et_3SiO group compared to the Me_3SiO group. This entropic effect makes the stability difference between the apical and equatorial isomers smaller for **6** than for **3** [$K(\mathbf{6}) < K(\mathbf{3})$]. Bentrude^[38] and Roberts^[39,40] have independently shown that the stereopermutation between ligands in apical and equatorial positions occurs by the M_4 mode^[41,42] through intermediates of σ^* geometry.^[43] The A factor, being lower than 10^{13} s^{-1} , is indicative of strong steric hindrance in the transition state along the pathway to the intermediate of σ^* geometry (Scheme 7). In fact, the radical goes from a TBP geometry, in which the bond angle between the bulky apical groups is close to 180° and the steric interaction is weak, to the more hindered tetrahedral σ^* geometry, in which all of the bond angles are close to 109° . The $E_{\text{a,exc}}$ values are close to those reported for other phosphoranyl radicals.^[33,37]

Reactivity of 3, 5, and 6

General comments: The reactivities of phosphoranyl radicals have frequently been reviewed during the last three decades.^[2–11] It appears that the main decay processes are α - and β -fragmentations (Scheme 1a and b, respectively), which depend on the polarity of the system, the steric bulk of the attached groups, and the stability of the released radicals.^[2–11] Other decay processes involve additions to unsaturated substrates such as alkenes^[32] or nitroso groups,^[32] or electron transfer;^[44] the only example of a second-order homolytic $S_{\text{H}2}$ substitution has been reported in the case of a dialkyl disulfide (Scheme 8).^[45–47] This $S_{\text{H}2}$ reaction involves mono- or bicyclic persistent phosphoranyl radicals. The reaction is slow and depends on the steric bulk of both the phosphoranyl radical and the dialkyl disulfide.^[45–47]

When a solution of **8** and **12** is irradiated, homolysis of **8** gives the trialkylsilyloxy radical [Eq. (3)], which is scavenged by phosphite **12** [Eq. (4)] to yield the phosphoranyl radical **6**. Since the expected fragmentation decay reactions are operational [Eqs. (5)–(9)] the concentration of the radical **6** does not increase indefinitely but reaches a stationary state. Then, when the light is switched off, the decay of **6** [Eq. (5)] is observed. As expected for fragmentation reac-

tions,^[4-9] a first-order decay is observed ($t_{1/2} = 270$ s for an irradiation time of 20 min; $T = 293$ K). However, when the same solution is irradiated for several hours, an unexpected increase in the half-life time is observed ($t_{1/2} = 759$ s; $T = 293$ K). This is a characteristic feature of a pseudo-first-order decay. Due to the high purity of the reactants and the solvent, *n*-hexane being assumed inert to H-abstraction by phosphoranyl radicals, reactions with impurities could be ruled out. The reaction of **6** with an excess of **12** [Eq. (6)] could also be disregarded because no significant change in the apparent decay rate constant k_d was observed when the concentration of **12** was varied from 0.05 M to 0.6 M ($[8] = 0.1$ M).^[48] The self-termination reaction of **6** [Eq. (7)] was also disregarded because such a reaction is generally only observed at low temperatures due to the formation of a very weak P–P bond.^[49,50]



For **3**: R = Me, R' = *i*Pr; for **5**: R = R' = Et; for **6**: R = Et, R' = *i*Pr.

S_{H2} homolytic substitution: Extensive studies of the evolution of the pseudo-first-order decay rate constant k_d for **3**, **5**, and **6** in the presence of **7** or **8** have revealed a linear increase of k_d with increasing concentration of the peroxides **7** and **8** (Figure 5). The same behaviour was observed when the study was carried out in the temperature range 273–313 K (Table 3).

When the light was switched off, only the decay reactions occurred [Eqs. (5) and (8), Eq. (9) being disregarded, vide infra]. Thus, if [per] denotes the concentration of peroxides **7** and **8**, and [P[•]] denotes the concentration of phosphoranyl radicals **3**, **5**, and **6**, the evolution of P[•] is given by Equations (10) and (11). The pseudo-first-order decay rate constant, k_d [Eq. (12)], is composed of the first-order decay rate constants, k_f , for the fragmentation reactions [Eq. (5)] and the second-order rate constant, k_{SH2} , for the homolytic substitution reaction [Eq. (8)].

$$-\frac{d[\text{P}^\cdot]}{dt} = k_f \cdot [\text{P}^\cdot] + k_{\text{SH2}} \cdot [\text{per}] \cdot [\text{P}^\cdot] \quad (10)$$

$$-\frac{d[\text{P}^\cdot]}{dt} = (k_f + k_{\text{SH2}} \cdot [\text{per}]) \cdot [\text{P}^\cdot] \quad (11)$$

$$k_d = k_f + k_{\text{SH2}} \cdot [\text{per}] \quad (12)$$

In Figure 5 and Table 3, the non-zero y-intercepts may be

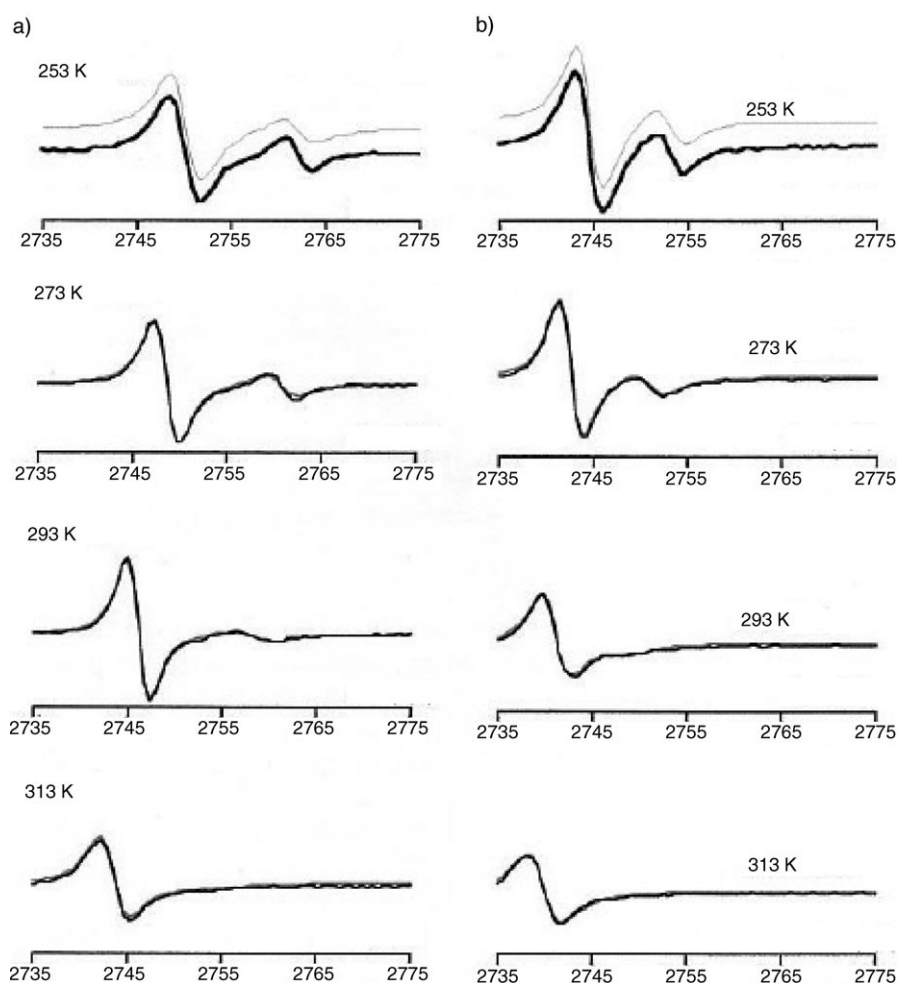


Figure 3. Temperature dependence of the low-field line (a) of **3** and (b) of **6**. The bold lines represent the experimental spectra and the thin lines the calculated spectra; field in gauss (G).

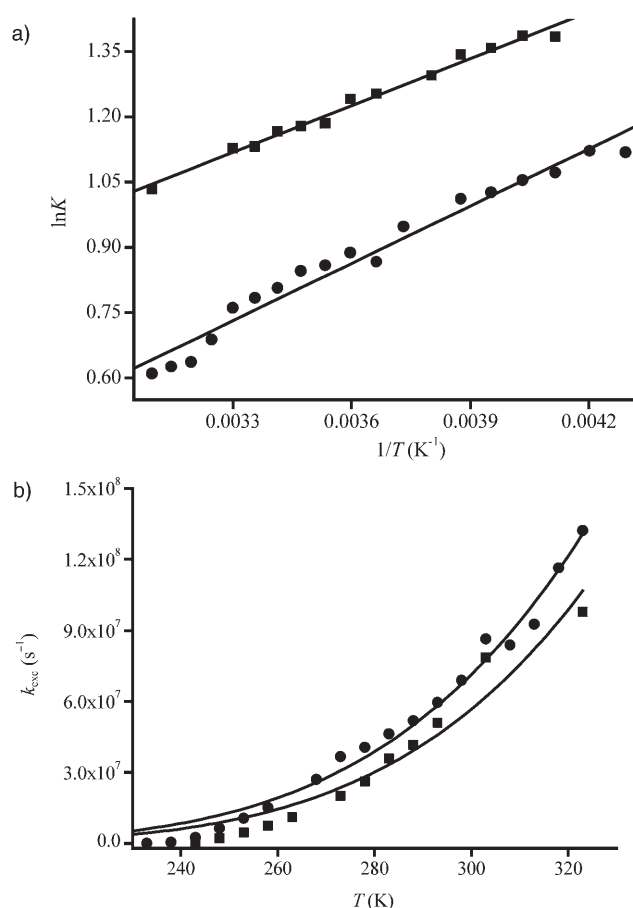


Figure 4. a) Van't Hoff plots for **3** (■) and **6** (●). b) Arrhenius plots for **3** (■) and **6** (●).

ascribed to first-order processes (vide infra) with the rate constants k_f , and the slopes may be ascribed to the second-order process with the rate constant k_{SH2} . As expected, k_{SH2} increases with decreasing bulkiness of the phosphoranyl radicals: the less hindered the radical centre (steric hindrance is expected to decrease in the series $iPr_3SiO > Et_3SiO > Me_2SiO$, that is, **6** > **3** > **5**), the less hampered the approach of the peroxide to the reactive centre.

The frequency factors, A_{SH2} , and the activation energies, $E_{a,SH2}$, were determined for **3**, **5**, and **6** (Figure 6a) and are reported in Table 4. Because of the small number of temperatures, and the $A-E_a$ compensation error effect,^[51] the Arrhenius parameters are not sufficiently accurate and reliable to allow a quantitative discussion; an increase of A_{SH2} with

decreasing steric hindrance in the series **5** < **3** < **6** would be expected (Table 4). However, the values of A_{SH2} are notably low ($\Delta S^\ddagger \approx -130 \text{ J mol}^{-1} \text{ K}^{-1}$), which is typical of reactions for which the approach of the reactant is hampered by the presence of bulky groups around the reactive centre.^[52]

As mentioned above, such an S_{H2} reaction has only been reported in the case of a dialkyl disulfide (Scheme 8).^[45,46] In these papers, Bentrude briefly mentioned the very fast reactions between persistent phosphoranyl radicals and dialkyl peroxides, which were suggested to occur by single-electron transfer (SET).^[45,46] At this stage, SET [Eq. (9)] cannot be rigorously excluded, even if its occurrence is unlikely. Outer-sphere SET should not be favored by a solvent such as *n*-hexane. Inner-sphere SET would be expected to be very fast and insensitive to steric hindrance, whereas k_{SH2} increases by a factor of six on going from **6** to **5**.^[44,53]

α -Fragmentation reactions of **3, **5**, and **6**:** In most cases, fragmentation reactions, namely α -scission (Scheme 1a) and β -scission (Scheme 1b), are regioselective (occurring at apical and equatorial positions, respectively) and chemoselective.^[4,7-9] Thus, the values of k_f (non-zero y -intercept) strongly depend on the nature of the groups involved in the fragmentation: $k_f(\mathbf{6}) < k_f(\mathbf{3}) < k_f(\mathbf{5})$. Therefore, a kinetic treatment of the data should differentiate between the two possibilities. Thus, the decay of **6** was used as a model (Scheme 9) with the apical **A** and equatorial **E** isomers in equilibrium (K), k'_i and k'_e as rate constants for the α -scission of iPr_3SiO and Et_3SiO groups, respectively, in apical positions, and k_i and k_e as rate constants for the β -scission of iPr_3SiO and Et_3SiO groups, respectively, in equatorial positions.

For fragmentations, the time evolution of $[P^*]$ is given by Equation (13), which is expressed in rearranged form in Equation (14), and using the relationships $[P^*] = [A] + [E]$, $K = [E]/[A]$ yields Equation (15).

$$-\frac{d[P^*]}{dt} = -\frac{d[A]}{dt} - \frac{d[E]}{dt} = k_f \cdot [P^*] \quad (13)$$

$$-\frac{d[P^*]}{dt} = 2k_i \cdot [A] + k'_i \cdot [A] + k'_e \cdot [A] + 2k'_i \cdot [E] + k_i \cdot [E] + k_e \cdot [E] = k_f [P^*] \quad (14)$$

$$-\frac{d[P^*]}{dt} = \frac{1}{1+K} (2k_i + k'_i + k'_e + 2k'_i K + k_i K + k_e K) \cdot [P^*] = k_f \cdot [P^*] \quad (15)$$

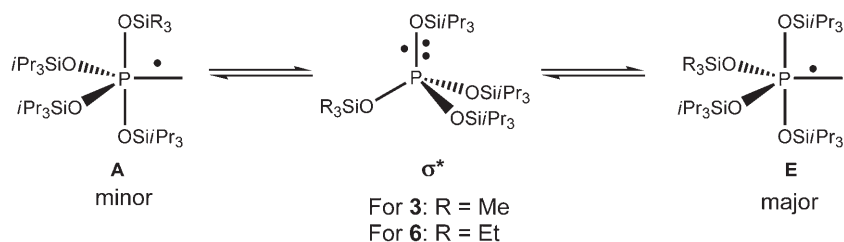
Table 2. Van't Hoff (free enthalpy ΔG_{exc} , enthalpy ΔH_{exc} , and entropy ΔS_{exc} for exchange) and Arrhenius (exchange frequency factor A_{exc} and activation energy $E_{a,exc}$) parameters for phosphoranyl radicals **3** and **6**.

Radicals	$\Delta G_{exc}^{[a]}$ [kJ mol ⁻¹]	ΔH_{exc} [kJ mol ⁻¹]	ΔS_{exc} [J K ⁻¹ mol ⁻¹]	$K^{[a]}$	A_{exc} [s ⁻¹]	$E_{a,exc}^{[a]}$ [kJ mol ⁻¹]
3 ^[b]	-2.9	-3.0 (±0.1)	-0.5 (±0.4)	3.29	(4.1±3.3) × 10 ¹¹	22.1 (±2.1)
6 ^[c]	-1.9	-3.7 (±0.2)	-6.0 (±0.6)	2.22	(3.6±1.4) × 10 ¹¹	21.3 (±1.0)

[a] At 293 K. [b] For Equation (1): $R^2 = 0.986$, $s = 0.014$, $n = 13$. For Equation (2): $R^2 = 0.94$. [c] For Equation (1): $R^2 = 0.968$, $s = 0.03$, $n = 18$. For Equation (2): $R^2 = 0.98$.

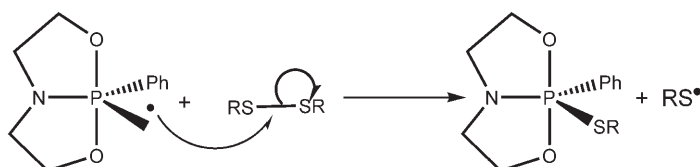
$$\frac{1}{1+K} (2k_i + k'_i + k'_e + 2k'_i K + k_i K + k_e K) = k_f \quad (16)$$

Thus, k_f depends on k'_i , k'_e , k_i , k_e , and K and is given by Equation (16). As k_i and k'_i are



Scheme 7. Chemical exchange between the apical **A** and equatorial **E** conformers of phosphoranyl radicals **3** and **6**.

unknown [K values have been determined above and (k_e , k'_e) values are given by k_f (**5**)], they exist only if the inequality Equation (17) holds, which is only fulfilled for positive equilibrium constants K [Eq. (18)]. This condition is only met if $k_f - k_e > 0$, which involves only



Scheme 8. Homolytic S_{H2} radical substitution of a dialkyl disulfide with a phosphoranyl radical.

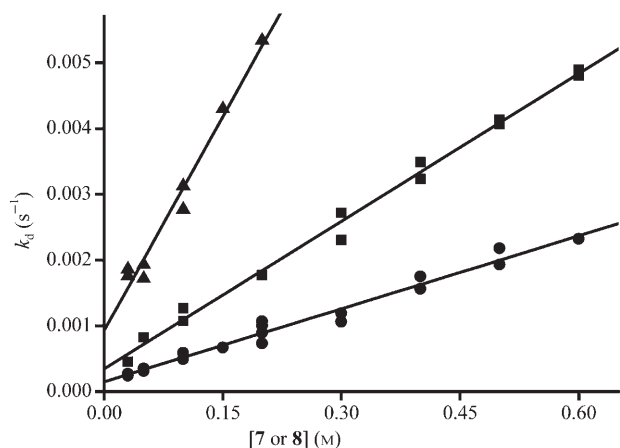


Figure 5. Evolution of k_d with the concentration of **7** and **8** for phosphoranyl radicals (0.3M): **3** (■), **5** (▲), and **6** (●) at 293 K.

Table 3. Fragmentation rate constants k_f and second-order homolytic substitution rate constants k_{SH2} between 273 K and 313 K for phosphoranyl radicals **3**, **5**, and **6** in the concentration range 0.025–0.6 M.

Radical	T [K]	k_f [$10^{-5} s^{-1}$]	k_{SH2} [$10^{-4} L mol^{-1} s^{-1}$]	$n^{[a]}$	R^2 [b,c]	$s^{[d]}$
3	273	6.3 ± 3.8	21.4 ± 1.1	8	0.98	6×10^{-5}
	283	41.6 ± 9.2	31.8 ± 3.7	5	0.96	10^{-4}
	293	34.4 ± 7.1	74.9 ± 1.9	13	0.99	10^{-4}
	303	47.1 ± 22.6	113.3 ± 8.0	7	0.97	4×10^{-4}
5	273	38.0 ± 1.7	12.8 ± 1.0	4	0.99	8×10^{-5}
	283	66.1 ± 7.2	48.5 ± 3.8	4	0.99	8×10^{-5}
	293	92.8 ± 15.3	216.7 ± 14.5	8	0.97	2×10^{-4}
	303	230.0 ± 60.4	285.7 ± 43.6	5	0.94	6×10^{-5}
6	273	3.1 ± 3.0	8.9 ± 1.3	7	0.90	6×10^{-5}
	293	14.8 ± 4.3	37.0 ± 1.4	18	0.97	10^{-4}
	303	21.0 ± 1.1	55.9 ± 3.7	8	0.97	2×10^{-4}
	313	36.0 ± 0.5	111.3 ± 1.5	5	0.99	6×10^{-5}

[a] Number of data. [b] Square of the linear regression coefficient. [c] All of the data give a Student t -test value in excess of 99.28% and in seven cases above 99.99%. [d] Standard deviation.

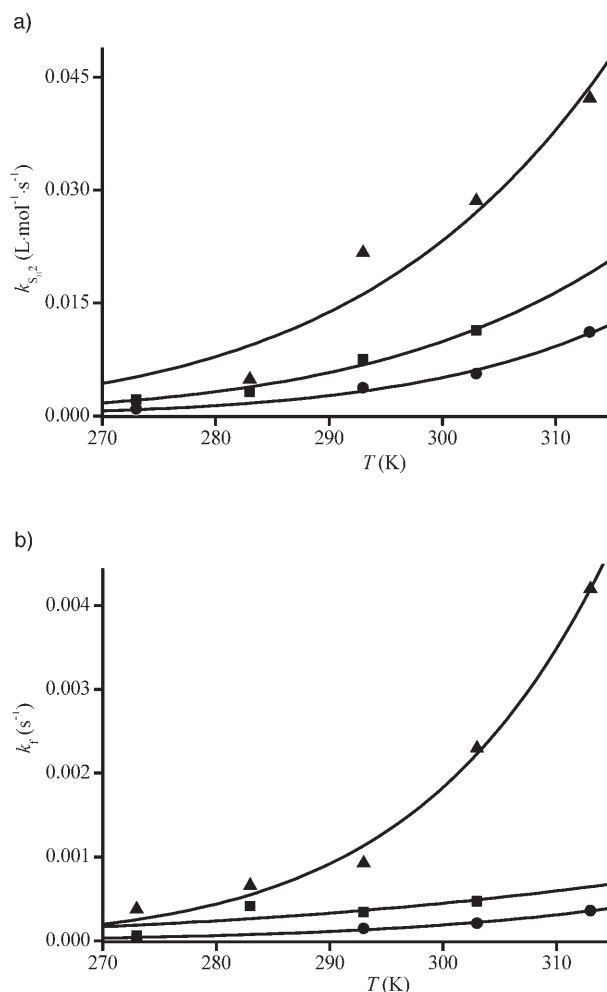
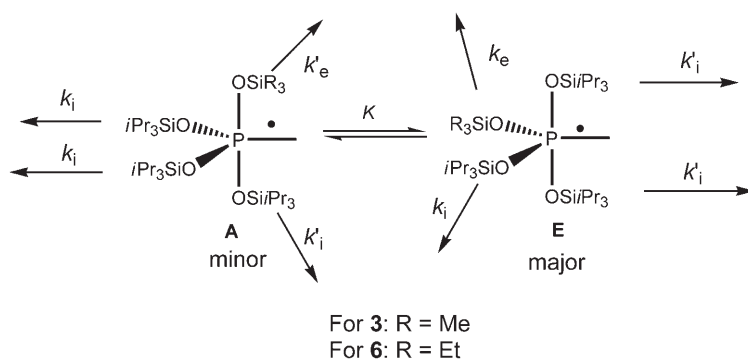


Figure 6. Arrhenius plots of: a) the second-order homolytic substitution rate constants k_{SH2} and b) the fragmentation rate constants k_f for phosphoranyl radicals **3** (■), **5** (▲), and **6** (●) in the temperature range 273–313 K.

Table 4. Arrhenius parameters for the fragmentation reaction (A_f , $E_{a,f}$) and for the second-order homolytic substitution reaction (A_{SH2} , $E_{a,SH2}$) for phosphoranyl radicals **3**, **5**, and **6**.

Radicals	$k_f^{[a]}$		$k_{SH2}^{[b]}$	
	A_f [s^{-1}]	$E_{a,f}$ [$kJ mol^{-1}$]	A_{SH2} [$L mol^{-1} s^{-1}$]	$E_{a,SH2}$ [$kJ mol^{-1}$]
3	$10^5 \pm 10^6$	35.9 ± 12.4	$(9.2 \pm 9) \times 10^4$	37.9 ± 8.5
5	$10^3 \pm 10^3$	49.9 ± 4.1	$(6.8 \pm 6.0) \times 10^4$	39.3 ± 5.3
6	800 ± 800	38.0 ± 4.0	$(5.6 \pm 5.0) \times 10^5$	46.2 ± 5.0

[a] For k_f , $R^2 = 0.957, 0.992$, and 0.991 for **3**, **5**, and **6**, respectively. [b] For k_{SH2} , $R^2 = 0.939, 0.981$, and 0.991 for **3**, **5**, and **6**, respectively.

Scheme 9. α -Scission versus β -scission.

the rate constant k_e related to the β -scission.

$$(2 + K)k_i + (2K + 1)k'_i = (1 + K)k_f - k_e K - k'_e > 0 \quad (17)$$

$$K = \frac{k_e k_f - k'_i}{k_f - k_e} > 0 \quad (18)$$

$$K \geq \frac{k_e k_f - k'_i}{k_f} \quad (19)$$

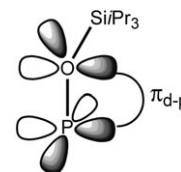
Assuming that α - and β -scissions occur simultaneously with the same rate constants, that is, $k_e = k'_e = 23.2 \text{ s}^{-1}$ (18.8 s^{-1} when errors are taken into account; Table 3), $k_f - k_e > 0$ does not hold.^[54] However, the inequality $k_f - k_e > 0$ holds when the α -scission is assumed to be the only fragmentation that occurs, and k'_e is given as $k_f(\mathbf{5})/2$. It was then checked that Equation (18) held for K , k_f , and k'_e values at various temperatures (Table 3); the K values given by Equation (18) are 3.8, 2.2, 2.1, 2.0, and 4.9, as compared with experimental K values of 2.4, 2.4, 2.2, 2.1, and 1.9 at 273 K, 283 K, 293 K, 303 K, and 313 K, respectively. The same approach and assumptions were then applied in the case of **3**, and the values of the α -scission rate constant k_m for the Me_3SiO group were obtained as $(58 \pm 23) \times 10^{-5} \text{ s}^{-1}$, $(175 \pm 51) \times 10^{-5} \text{ s}^{-1}$, $(134 \pm 30) \times 10^{-5} \text{ s}^{-1}$, and $(145 \pm 106) \times 10^{-5} \text{ s}^{-1}$ at 273 K, 283 K, 293 K, and 303 K, respectively. It is interesting to note that the α -scission pathway is chemoselective [Eq. (19)], with release of the Me_3SiO group. This is contrary [Eq. (20)] to the expected process, in which release of the bulkier $i\text{Pr}_3\text{SiO}$ group should be faster than release of the less sterically demanding Me_3SiO group because of the larger relief of steric strain.

$$i\text{Pr}_3\text{SiO} \ll \text{Et}_3\text{SiO} < \text{Me}_3\text{SiO} \quad (20)$$

Stabilizing $\pi_{\text{d-p}}$ interactions are known in phosphoranyl chemistry,^[32] and they have been invoked to rationalize the observed reactivities of phosphites^[55] and phosphoranes.^[32] Thus, the steric hindrance of a bulky group can force the oxygen lone pairs to adopt a specific conformation in which there are $\pi_{\text{d-p}}$ interactions between the p-type lone pair and the d_{xy} or $d_{x^2-y^2}$ orbitals of the phosphorus atom. Such stabilizing interactions overcome the steric hindrance of the

bulky groups. Thus, they confer a double-bond character to the P–O bond (Scheme 10).

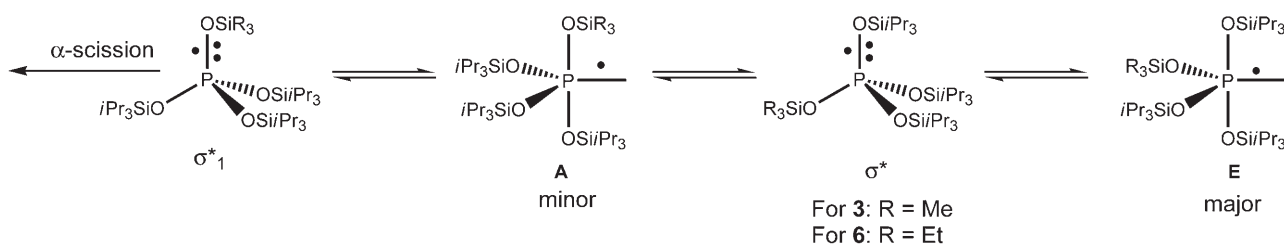
The frequency factors, A_f , and the activation energies, $E_{\text{a,f}}$, were determined for **3**, **5**, and **6** (Figure 6a) and are reported in Table 4. For the same reasons as above, the Arrhenius parameters are not sufficiently accurate and reliable to allow a quantitative discussion. In general, A values for fragmentation reactions^[52] are clearly above 10^{13} s^{-1} , that is, $\Delta S^\ddagger >$

Scheme 10. Possible $\pi_{\text{d-p}}$ interactions.

$0 \text{ J mol}^{-1} \text{ K}^{-1}$, because of the strain relief and the increased motion on going from one to two molecules. In spite of the large errors, the A_f values ($\Delta S^\ddagger < -130 \text{ J mol}^{-1} \text{ K}^{-1}$) are well below 10^{13} s^{-1} , which is indicative of very restricted conformational changes or strong steric strain in reaching the transition state. This trend is contrary to expectation: $A_f(\mathbf{6}) < A_f(\mathbf{3}) < A_f(\mathbf{5})$. Furthermore, the $E_{\text{a,f}}$ values are lower than expected considering the BDE of the P–O bond. The $E_{\text{a,f}}$ is lowered because the trialkylsilyloxy radical released by α -scission is probably strongly stabilized by a π -interaction between the SOMO and the available d orbitals on the silicon atom.^[56–58] Such an α -scission of P–O, releasing a stabilized radical, has been reported for the release of phenoxyl radical from the phosphoranyl radical $(t\text{BuO})_3\text{P}^\bullet$.^[7,59–61]

Roberts and Singh reported that α -scission occurs through an intermediate of σ^* geometry with the odd electron localized in the antibonding orbital of the P–O bond.^[37] Therefore, the α -scission should occur through an intermediate of σ^* geometry with the odd electron localized in the P–O bond of the P–OSiEt₃ moiety. As noted above, the conversion from a TBP to a σ^* geometry for the chemical exchange is entropically disfavored ($\Delta S^\ddagger = -30 \text{ J mol}^{-1} \text{ K}^{-1}$). Thus, the conversion from isomer **A** to intermediate σ^*_1 (Scheme 11) is probably more disfavored, that is, A_f is small because of strong steric hindrance between the three $i\text{Pr}_3\text{SiO}$ groups and because of the double-bond character of the P–O bond ($\pi_{\text{d-p}}$ interaction; Scheme 10), which is expected to hamper the conformational change.

Reactivity of 1: It was not possible to carry out extensive studies on the influence of the concentration of **7** on **1** because a very fast oxidation of $\text{P}(\text{OSiMe}_3)_3$ to $\text{O}=\text{P}(\text{OSiMe}_3)_3$ occurs by reaction with **7**.^[62] Kinetic experiments performed at 253 K with concentrations of **7** of 0.2 M, 0.3 M, and 0.4 M afforded k_d values of 0.06 s^{-1} , 0.17 s^{-1} , and 0.48 s^{-1} , respectively, showing the same trend as reported above. Hence, it was



Scheme 11. Intermediates involved in the α -scission/chemical exchange processes.

possible to determine a rough value of $2.1 \text{ L mol}^{-1} \text{ s}^{-1}$ for k_{SH_2} , which is three orders of magnitude larger than the k_{SH_2} measured in the range 273–293 K for **3**, **5**, and **6**.^[63] Significantly, the k_d values for **1** at 253 K are as large as those for **5** at 313 K, indicating very easy access of **7** to the reactive centre, and probably also a very easy α -scission of the Me_3SiO group as expected. Hence, assuming a twofold increase of k_d by an increment of 10 K, k_d at 293 K is roughly 1 s^{-1} and hence $t_{1/2} < 1 \text{ s}$. Therefore, **5**, **3**, and **6** are roughly 140, 340, and 770 times more persistent than **1**.

Conclusion

We have developed the first persistent noncyclic phosphoranyl radicals. The main decay pathway has been identified as an $S_{\text{H}2}$ reaction between the phosphoranyl radical and a peroxide. The $t_{1/2}$ of 35 min at 293 K is at least 10^6 times longer than those observed for noncyclic phosphoranyl radicals, and around 10^3 times longer than those reported for the most persistent phosphoranyl radical hitherto ever observed.^[4,7,8] If the $S_{\text{H}2}$ reaction were to be suppressed, a $t_{1/2}$ of around 77 min should be observed for radical **6**. Furthermore, the spectroscopic properties of these radicals are well suited for the observation of enhanced DNP effects.^[18] Hence, although the preparation of a persistent phosphoranyl radical remains a very difficult objective to achieve, it is no longer an inaccessible one.^[14]

Experimental Section

The reagents diazabicyclo[2.2.2]octane (DABCO), chlorotrimethylsilane, chlorotriethylsilane, chlorotriisopropylsilane, tris(trimethylsilyl) phosphite, and sodium were purchased from Aldrich and used as received. Pyridine, triethylamine, hexane, toluene, benzene, and phosphorous acid were purchased from Aldrich and were purified by conventional procedures.^[64] Cyclopropane was purchased from Messer Griesheim GmbH. DABCO-hydrogen peroxide complex (DABCO·2H₂O₂) was prepared as described by Ricci et al.^[65] Bis(trimethylsilyl) peroxide (**7**) and bis(triethylsilyl) peroxide (**8**) were prepared as reported in the literature.^[20,65] NMR spectra were recorded on Bruker AC-100 (³¹P 40.3 MHz), Bruker AC-200 (¹H 200.13 MHz and ¹³C 50.36 MHz), and Bruker AMX-400 spectrometers (²⁹Si 79.8 MHz) at the “Spectropole” in Marseille. Chemical shifts are referenced to TMS (internal reference) for ¹H and ²⁹Si NMR spectra, to the carbon of the deuterated solvent (internal reference) for ¹³C NMR spectra, and to 85% H₃PO₄ (external reference) for ³¹P NMR spectra. Elemental analyses were also performed at the “Spectropole” in Marseille.

Bis(trimethylsilyl) peroxide (7): Yield: 30%, b.p.: 38–42 °C/20 mbar.^[20] ¹H NMR (CDCl₃): $\delta = 0.18 \text{ ppm}$; ¹³C NMR (CDCl₃): $\delta = -1.24 \text{ ppm}$; ²⁹Si NMR (CDCl₃): $\delta = 27.60 \text{ ppm}$; ^{66]} elemental analysis calcd (%) for C₆H₁₈O₂Si₂ (178.08): C 40.40, H 10.17; found: C 40.35, H 10.49.

Bis(triethylsilyl) peroxide (8): Yield: 60%, b.p.: 65 °C/1 mbar.^[20] ¹H NMR (C₆D₆): $\delta = 0.73 \text{ (q, } ^3J = 8.0 \text{ Hz, 12 H; CH}_2\text{)}, 1.04 \text{ (t, } ^3J = 8.0 \text{ Hz, 18 H; CH}_3\text{)}$; ¹³C NMR (C₆D₆): $\delta = 4.31 \text{ (CH}_2\text{)}, 7.07 \text{ ppm (CH}_3\text{)}$; ¹³C NMR (CDCl₃): $\delta = 3.98 \text{ (CH}_2\text{)}, 6.60 \text{ ppm (CH}_3\text{)}$; ²⁹Si NMR (CDCl₃): $\delta = 28.22 \text{ ppm}$; elemental analysis calcd (%) for C₁₂H₃₀O₂Si₂ (262.18): C 54.90, H 11.52; found: C 54.88, H 11.55.^[67]

Bis(triethylsilyl)phosphonate (**9**) and bis(triisopropylsilyl)phosphonate (**10**) were prepared by an adaptation of the procedure of Sekine et al.^[23] At 0 °C, under a nitrogen atmosphere, dry triethylamine (2 equiv) was added dropwise to a solution of the requisite chlorotrialkylsilane (2 equiv) and dry phosphorous acid (1 equiv) in dry pyridine. The solution was stirred for 24 h at room temperature, in the course of which it became light orange in color. A white precipitate formed, which was filtered off. The pyridine was distilled off under reduced pressure to leave a dark orange oil, which was distilled under reduced pressure to yield a colorless oil.

Bis(triethylsilyl) phosphonate (9): B.p. 90–130 °C/0.03 mbar, yield 48%.^[68] ¹³C NMR (CDCl₃): $\delta = 5.36 \text{ (} ^2J(\text{P,C}) = 1.3 \text{ Hz; CH}_2\text{)}, 6.27 \text{ ppm (CH}_3\text{)}$; ³¹P NMR (CDCl₃): $\delta = -15.3 \text{ ppm (} ^1J(\text{P,H}) = 693.0 \text{ Hz)}$; ²⁹Si NMR (CDCl₃): $\delta = 24.8 \text{ ppm (} ^2J(\text{P,Si}) = 8.6 \text{ Hz)}$.

Bis(triisopropylsilyl) phosphonate (10): B.p. 135–155 °C/0.03 mbar, yield 86%. ¹³C NMR (CDCl₃): $\delta = 12.43 \text{ (} ^2J(\text{P,C}) = 1.5 \text{ Hz; CH)}, 17.46 \text{ ppm (CH}_3\text{)}$; ³¹P NMR (CDCl₃): $\delta = -7.1 \text{ ppm (} ^1J(\text{P,H}) = 694.0 \text{ Hz)}$; ²⁹Si NMR (CDCl₃): $\delta = 21.0 \text{ ppm (} ^2J(\text{P,Si}) = 12.0 \text{ Hz)}$; elemental analysis calcd (%) for C₁₈H₄₅O₃PSi₂ (394.25): C 54.78, H 11.98; found: C 54.72, H 11.98.

Tris(trimethylsilyl) phosphite (**11**) and tris(triisopropylsilyl) phosphite (**12**) were prepared by an adaptation of the procedure of Sekine et al.^[23] Under a nitrogen atmosphere, sodium (0.3 equiv) was added to the neat bis(trialkylsilyl) phosphonate (1 equiv). The mixture was heated for 24 h at 150 °C for **11** and at 210 °C for **12**. The grey-brown-green mixture was purified first by kugelrohr distillation to afford a colorless oil, which was then distilled under reduced pressure.

Tris(trimethylsilyl) phosphite (11): Kugelrohr distillation, $T = 160 \text{ °C/} 0.03 \text{ mbar}$, b.p. 130–134 °C/1 mbar,^[69] yield 33%.^[70,71] ¹H NMR (C₆D₆): $\delta = 0.75 \text{ (poorly resolved q, } ^3J(\text{H,H}) = 8.0 \text{ Hz, 18 H; CH}_2\text{)}, 1.06 \text{ ppm (poorly resolved t, } ^3J(\text{H,H}) = 7.0 \text{ Hz, 27 H; CH}_3\text{)}$; ¹³C NMR (C₆D₆): $\delta = 6.53 \text{ (} ^2J(\text{P-C}) = 1.8 \text{ Hz; CH}_2\text{)}, 7.04 \text{ ppm (} ^4J(\text{P,C}) = 1.5 \text{ Hz; CH}_3\text{)}$; ³¹P NMR (C₆D₆): $\delta = 111.0 \text{ ppm}$; ²⁹Si NMR (C₆D₆): $\delta = 15.75 \text{ ppm (} ^2J(\text{P,Si}) = 8.6 \text{ Hz)}$; elemental analysis calcd (%) for C₁₈H₄₅O₃PSi₃ (424.78): C 50.89, H 10.67; found: C 50.78, H 10.87. Note: This compound is highly sensitive to hydrolysis.^[68–71]

Tris(triisopropylsilyl) phosphite (12): Kugelrohr distillation, $T = 200 \text{ °C/} 0.03 \text{ mbar}$, b.p. 160–180 °C/0.03 mbar, yield 42%. ¹³C NMR (CDCl₃): $\delta = 13.30 \text{ (CH)}, 18.00 \text{ ppm (} ^4J(\text{P,C}) = 2.3 \text{ Hz; CH}_3\text{)}$; ³¹P NMR (CDCl₃): $\delta = 107.9 \text{ ppm}$; ²⁹Si NMR (CDCl₃): $\delta = 12.4 \text{ ppm (} ^2J(\text{P,Si}) = 14.0 \text{ Hz)}$; elemental analysis calcd (%) for C₂₇H₆₃O₃PSi₃ (550.38): C 58.85, H 11.52; found: C 58.86, H 11.51.

EPR experiments: EPR spectra were recorded on a Bruker ESP 300 spectrometer, equipped with an HP 5350 B frequency meter and an NMR

gaussmeter. The sample temperature was controlled with an ER4111 VT temperature controller unit. UV-irradiation was provided by a high-pressure 1000 W Xe-Hg arc lamp with the beam focused through Suprasil lenses. The experiments were performed in *n*-hexane, toluene, benzene, and cyclopropane as solvents. The EPR probes were degassed by repeated freeze–pump–thaw cycles on a high vacuum line (10^{-5} mbar). The EPR probes were made of Suprasil[®] quartz with o.d. 5 mm and were filled with 0.5 mL of the sample solution and irradiated with the light power set at 600 W.

Kinetic experiments: Evolution of the growth (light on) and the decay (light off) of the phosphoranyl radicals was monitored on the EPR spectrometer either by the profile method (the field is set at the top of the EPR line; suitable for $t_{1/2}$ decay in the range 5 s to 15 min) or by the double-integrals method (the line is recorded at even times and doubly integrated). The latter method is the most suitable for $t_{1/2} > 15$ min. Apparent absolute rate constants, k , for the decay were obtained by processing the data with an in-house nonlinear square regression Domino program. The values of k_{exc} were determined with the fitting program of Prof. A. Rockenbauer.^[28] EPR spectra were fitted one at a time at different temperatures using as fitting parameters for both isomers a_{P} , ΔH_{EPR} for each line, isomer population, and the rate constants k_1 and k_{-1} for each elementary reaction of the equilibrium. The values of k_{exc} were then given as $k_{\text{exc}} = k_1 + k_{-1}$.

Acknowledgements

The authors are grateful to the Université de Provence, the CNRS, and the Délégation Générale à l'Armement (DGA) for their financial support. SRAM thanks the CNRS and the DGA for a three-year fellowship.

- [1] J. K. Kochi, P. J. Krusic, *J. Am. Chem. Soc.* **1969**, *91*, 3944–3946.
- [2] A. G. Davies, D. Griller, B. P. Roberts, *Angew. Chem.* **1971**, *83*, 800–801; *Angew. Chem. Int. Ed.* **1971**, *10*, 738–739. The phosphoranyl radicals were first suggested in: F. Ramirez, N. McElvie, *J. Am. Chem. Soc.* **1957**, *79*, 5829–5830.
- [3] C. Walling, M. S. Pearson, *Top. Phosphorus Chem.* **1966**, *3*, 1–56.
- [4] W. G. Bentrude in *Free Radicals*, vol. 2 (Ed.: J. K. Kochi), Wiley-Interscience, New York, **1973**, pp. 595–664.
- [5] P. Shipper, E. H. J. M. Janzen, H. M. Buck, *Top. Phosphorus Chem.* **1977**, *191*, 407–503.
- [6] S. P. Solodnikov, N. N. Bubnov, A. I. Prokof'ev, *Russ. Chem. Rev.* **1980**, *49*, 1–13.
- [7] B. P. Roberts in *Advances in Free Radical Chemistry*, vol. 6 (Ed.: G. H. Williams), Heyden and Son, London, **1980**, pp. 225–289.
- [8] W. G. Bentrude, *Acc. Chem. Res.* **1982**, *15*, 117–125.
- [9] W. G. Bentrude, in *Reactive Intermediates*, vol. 3 (Ed.: R. A. Abramovitch), Plenum Press, London, **1983**, pp. 199–298.
- [10] W. G. Bentrude, in *The Chemistry of Organophosphorus Compounds*, vol. 1 (Ed.: F. R. Hartley), Wiley, Chichester, **1990**, pp. 531–566.
- [11] S. Marque, P. Tordo, *Top. Curr. Chem.* **2005**, *250*, 43–76.
- [12] D. Gimes, D. Bertin, S. Marque, O. Guerret, P. Tordo, *Tetrahedron Lett.* **2003**, *44*, 1227–1229.
- [13] J. L. Hodgson, M. L. Coote, *J. Phys. Chem. A* **2005**, *109*, 10013–10021.
- [14] D. L. Haire, E. G. Janzen, G. Chen, V. J. Robinson, I. Hrvoic, *Magn. Reson. Chem.* **1999**, *37*, 251–258.
- [15] E. Belorizky, P. H. Fries, S. Rast, *C. R. Acad. Sci., Ser. IIC Chem.* **2001**, *4*, 825–832.
- [16] A. Abragam, *Phys. Rev.* **1955**, *98*, 1729–1735.
- [17] W. Müller-Marmuth, R. Meise-Gresch, *Adv. Magn. Reson.* **1983**, *1*, 11.
- [18] S. Marque, Y. Berchadsky, K. Lang, M. Moussavi, A. Fournel, P. Bertrand, J. Belorizky, P. Tordo, *J. Phys. Chem. A* **1997**, *101*, 5640–5645.
- [19] For Me₃Si-OMe: Y.-R. Luo, *Handbook of Bond Dissociation Energies in Organic Compounds*, CRC Press, Boca Raton, **2003**, p. 292.
- [20] For **7**: yield 35%, b.p. 42°C/40 mbar. For **8**: yield 71%, b.p. 61°C/0.05 mbar. P. G. Cookson, A. G. Davies, N. Fazal, *J. Organomet. Chem.* **1975**, *99*, C31–C32.
- [21] Et₃SiOH: ¹³C NMR (CDCl₃): $\delta = 5.8$ (CH₂), 6.55 ppm (CH₃); ²⁹Si NMR (CDCl₃): $\delta = 19.24$ ppm. Et₃SiOOH: ¹³C NMR (CDCl₃): $\delta = 3.63$ (CH₂), 6.85 ppm (CH₃); ²⁹Si NMR (CDCl₃): $\delta = 30.73$ ppm. (Et₃Si)₂O: ¹³C NMR (CDCl₃): $\delta = 6.3$ (CH₂), 6.7 ppm (CH₃); ²⁹Si NMR (CDCl₃): $\delta = 8.86$ ppm; b.p. 61°C/1 mbar. For (Et₃Si)₂O purchased from Aldrich: ¹³C NMR (CDCl₃): $\delta = 6.55$ (CH₂), 6.90 ppm (CH₃); ²⁹Si NMR (CDCl₃): $\delta = 8.89$ ppm.
- [22] Et₃SiOH: ²⁹Si NMR (CDCl₃): $\delta = 19.3$ ppm. (Et₃Si)₂O: ²⁹Si NMR (CDCl₃): $\delta = 9.11$ ppm. H. Marsmann in *Basic Principles and Progress, ²⁹Si-NMR Spectroscopic Results* (Eds.: P. Dhiel, E. Fluck, R. Kosfeld), Springer, Heidelberg, **1986**, pp. 153–233.
- [23] M. Sekine, K. Akimoto, K. Yamada, T. Hata, *J. Org. Chem.* **1981**, *46*, 2097–2107.
- [24] V. M. D'yakov, M. G. Voronkov, N. F. Orlov, *Bull. Acad. Sci. USSR Div. Chem. Sci. (Engl. Transl.)* **1972**, *11*, 2417–2422.
- [25] A. G. Davies, B. P. Roberts in *Landolt-Börnstein, Magnetic Properties of Free Radicals, New Series, Group 2, vol. 9* (Eds.: K. H. Hellwege, H. Fischer), Springer, Berlin, **1979**, Part c2, 215.
- [26] P. Tordo in *Landolt-Börnstein, Magnetic Properties of Free Radicals, New Series, Group 2, vol. 17* (Ed.: H. Fischer), Springer, Berlin, **1988**, Part e, 254.
- [27] S. R. A. Marque, P. Tordo in *Landolt-Börnstein, Magnetic Properties of Free Radicals, New Series, Group 2* (Ed.: H. Fischer), Springer, Berlin, in press.
- [28] A. Rockenbauer, L. Korecz, *Appl. Magn. Reson.* **1996**, *10*, 29–43.
- [29] P. W. Atkins, M. C. R. Symons, *The Structure of Inorganic Radicals*, Elsevier, **1967**, p. 238.
- [30] For (EtO)₃P' with TBP geometry, $\rho_{3p}/\rho_{3s} = 1.98$. C. M. L. Kerr, K. Webster, F. Williams, *J. Phys. Chem.* **1975**, *79*, 2650–2662.
- [31] For Ph₃P'SR with σ^* geometry, $\rho_{3p}/\rho_{3s} = 4.70$. J. C. Evans, S. P. Mishra, C. C. Rowlands, *Chem. Phys. Lett.* **1980**, *72*, 168–170.
- [32] D. Griller, B. P. Roberts, *J. Chem. Soc. Perkin Trans. 2* **1973**, 1416–1421.
- [33] J. A. Baban, B. P. Roberts, *J. Chem. Soc. Perkin Trans. 2* **1980**, 876–882.
- [34] A. G. Davies, D. Griller, B. P. Roberts, *J. Chem. Soc. Perkin Trans. 2* **1972**, 993–998.
- [35] J. W. Cooper, M. J. Parrott, B. P. Roberts, *J. Chem. Soc. Perkin Trans. 2* **1977**, 730–741.
- [36] Alkyl groups are considered as donor groups, $\sigma_{\text{IMe}} = \sigma_{\text{IEt}} = \sigma_{\text{IPr}} = -0.01$. M. Charton, *Prog. Phys. Org. Chem.* **1981**, *13*, 119–251.
- [37] B. P. Roberts, K. Singh, *J. Chem. Soc. Perkin Trans. 2* **1980**, 1549–1556.
- [38] A. Nakanashi, W. G. Bentrude, *J. Am. Chem. Soc.* **1978**, *100*, 6271–6273.
- [39] B. P. Roberts, K. Singh, *J. Chem. Soc. Chem. Commun.* **1979**, 980–981.
- [40] J. R. M. Giles, B. P. Roberts, *J. Chem. Soc. Perkin Trans. 2* **1981**, 1211–1220.
- [41] M. I. Musher, *J. Am. Chem. Soc.* **1972**, *94*, 5662–5665.
- [42] M. I. Musher, *J. Chem. Educ.* **1974**, *51*, 94–97.
- [43] W. G. Bentrude, M. Moriyama, H. D. Mueller, A. E. Sopchik, *J. Am. Chem. Soc.* **1983**, *105*, 6053–6061.
- [44] S. Yasui, *Trends Org. Chem.* **1995**, *5*, 141–149.
- [45] T. Kawashima, W. G. Bentrude, *J. Am. Chem. Soc.* **1979**, *101*, 3981.
- [46] W. G. Bentrude, T. Kawashima, B. A. Keys, M. Garroussian, W. Heide, D. A. Wedegaertner, *J. Am. Chem. Soc.* **1987**, *109*, 1227–1235.
- [47] M. Garroussian, W. G. Bentrude, G.-V. Rösenthaller, *J. Org. Chem.* **2001**, *66*, 6181–6184.
- [48] A similar observation has been reported for (RO)₃P' radicals: B. P. Roberts, J. C. Scaiano, *J. Chem. Soc. Perkin Trans. 2* **1981**, 905–911.
- [49] G. B. Watts, K. U. Ingold, *J. Am. Chem. Soc.* **1972**, *94*, 2528–2529.

- [50] BDE(R_f PPR₄) is expected to be much smaller than 240 kJ mol⁻¹; see reference [4].
- [51] K. Héberger, S. Kemény, T. Vidoczy, *Int. J. Chem. Kinet.* **1987**, *19*, 171–181.
- [52] S. W. Benson, *Thermochemical Kinetics*, John Wiley and Sons, New York, **1968**.
- [53] J. A. Kampmeier, T. W. Nalli, *J. Org. Chem.* **1993**, *58*, 943–949.
- [54] It is assumed that the fragmentation of the Et₃SiO group is influenced by the presence of *i*Pr₃SiO. Indeed, if the α - and β -scissions are assumed to be independent of the trialkylsilyl groups and of the position, the same k_f values should be observed for **5** and **6**, which is not the case (Table 3). Therefore, the *i*Pr₃SiO group gives rise to very different reactivity compared to the Et₃SiO group. Then, assuming a preferential position for the fragmentation, one should have observed $k_f(\mathbf{6}) \approx k_f(\mathbf{5})/2$. The clearly smaller than expected value of $k_f(\mathbf{6})$ is due either to the equilibrium between the apical (**A**) and equatorial (**E**) forms of **6**, or to the steric hindrance generated by the presence of three bulky *i*Pr₃SiO groups. Nevertheless, the presence of bulky *i*Pr₃SiO groups does not enhance the fragmentation of the Et₃SiO group. However, this steric hindrance might be responsible for the small discrepancies between the calculated and experimental K values.
- [55] R. V. Hodges, F. A. Houle, J. L. Beauchamp, R. A. Montag, J. G. Verkade, *J. Am. Chem. Soc.* **1980**, *102*, 932–935.
- [56] J. A. Baban, J. P. Goddard, B. P. Roberts, *J. Chem. Soc. Perkin Trans. 2* **1986**, 1269–1274.
- [57] H. Kwart, K. G. King, *d-Orbitals in the Chemistry of Silicon, Phosphorus, and Sulfur*, Springer, Berlin, **1977**, pp. 2–17.
- [58] L. Olsson, G. H. Ottosson, D. Cremer, *J. Am. Chem. Soc.* **1995**, *117*, 1229–1251.
- [59] C. Walling, M. S. Pearson, *J. Am. Chem. Soc.* **1964**, *86*, 2262–2266.
- [60] W. G. Bentrude, *Tetrahedron Lett.* **1965**, *6*, 3543–3548.
- [61] K. Schwetlick, T. König, C. Ruger, J. Pionteck, *Z. Chem.* **1986**, *26*, 360–366.
- [62] Observed by ³¹P NMR and already reported in ref. [33].
- [63] The value of k_f is negative.
- [64] W. L. F. Armarego, C. L. L. Chai, *Purification of Laboratory Chemicals*, 5th ed., Butterworth Heinemann, Amsterdam, **2003**.
- [65] $\delta = 0.18$ ppm. M. Taddei, A. Ricci, *Synthesis* **1986**, 633–635.
- [66] $\delta = 27.2$ ppm. P. Babin, B. Benneteau, J. Dunoguès, *Synth. Commun.* **1992**, *22*, 2849–2852.
- [67] A. Simon, H. Arnold, *J. Prakt. Chem.* **1959**, *4*, 241–255.
- [68] M. G. Voronkov, V. A. Koloseva, V. N. Zgonnik, *Bull. Acad. Sci. USSR Div. Chem. Sci. (Engl. Transl.)* **1957**, *6*, 1381–1385.
- [69] For **9**: $J_{PH} = 690$ Hz. For **11**: δ (CCl₄) = 0.76 (CH₂), 0.97 (CH₃). M. G. Voronkov, N. F. Orlov, B. L. Kaufman, V. A. Pestunovich, *J. Gen. Chem. USSR* **1967**, *1*, 1958–1960.
- [70] Yield 32%. M. G. Voronkov, Y. Zkorik, *J. Gen. Chem. USSR* **1965**, *35*, 105–108.
- [71] Yield 71%. N. F. Orlov, E. V. Sudakova, *J. Gen. Chem. USSR* **1968**, *38*, 211.

Received: March 3, 2006
Published online: July 18, 2006